Compressed Sensing for MIMO Radar - Algorithms and Performance

Thomas Strohmer*
Dept. Mathematics
UC Davis
Davis CA 95616

Benjamin Friedlander [†]
Dept. Elec. Eng.
UC Santa Cruz
Santa Cruz, CA 95064

Abstract

Compressed sensing techniques make it possible to exploit the sparseness of radar scenes to potentially improve system performance. In this paper compressed sensing tools are applied to MIMO radar to reconstruct the scene in the azimuth-range-Doppler domain. Conditions are derived for the radar waveforms and the transmit and receive arrays so that the radar sensing matrix has small coherence and sparse recovery becomes possible. Theoretical performance bounds are presented and validated by numerical simulations.

1 Introduction

Two relatively recent developments in radar are the development of MIMO (multi-input multi-output) radar [9], and the application of compressed sensing to radar signal processing [10].

MIMO radar is characterized by using multiple antennas to simultaneously transmit diverse, usually orthogonal, waveforms in addition to using multiple antennas to receive the reflected signals. MIMO radar has the potential for enhancing spatial resolution and improving interference and jamming suppression. The ability of MIMO radar to shape the transmit beam post facto allows for adapting the transmission based on the received data in a way which is not possible in "conventional" radar.

Most radar scenes are sparse in the sense that only a small fraction of the range-azimuth or range-Doppler-azimuth cells are occupied by objects of interest. In fact in most situations this fraction is very small indeed. This sparsity assumption suggests to approach the MIMO radar problem using the framework of compressed sensing (CS) [3, 5]. In this paper we develop the basic theory needed to apply CS to MIMO radar. Some initial empirical results on waveform design for compressed sensing MIMO radar can be found in [4].

At the core of compressed sensing lies the discovery that it is possible to reconstruct a sparse signal $\mathbf{x}$ exactly from a underdetermined linear system of equations $\mathbf{Ax} = \mathbf{y}$ *and* that this can be done in a computationally efficient manner via ℓ_1-minimization, cf. [2, 3, 5]. More specifically, assume $\mathbf{x} \in \mathbb{C}^m$ is a signal that is sparse, i.e., the number of its non-zero components satisfies $s := \|\mathbf{x}\|_0 \ll m$ (where $\|\mathbf{x}\|_0 := \#\{k : x_k \neq 0\}$). Consider $\mathbf{Ax} = \mathbf{y}$, where $\mathbf{A}$ is an $n \times m$ matrix of rank n with $n < m$. Since this system is underdetermined, there are infinitely many solutions. Due to the sparsity of $\mathbf{x}$ one could compute $\mathbf{x}$ by solving the optimization problem

$$\min_{\mathbf{x}} \|\mathbf{x}\|_0 \quad \text{s.t.} \quad \mathbf{Ax} = \mathbf{y}. \tag{1}$$

However solving (1) is an NP-hard problem and thus practically not feasible. Instead we consider its convex relaxation (also known as *Basis Pursuit*)

$$\min_{\mathbf{x}} \|\mathbf{x}\|_1 \quad \text{s.t.} \quad \mathbf{Ax} = \mathbf{y}, \tag{2}$$

which can be solved efficiently via linear or quadratic programming techniques. It is by now well-known that under certain conditions on the matrix $\mathbf{A}$ and the sparsity of $\mathbf{x}$, both (1) and (2) have the same unique solution [2, 3, 5, 6]. One such condition is the restricted isometry property [2], which is satisfied for instance by Gaussian random matrices or random partial Fourier matrices. Another condition (utilized in this paper) is based on the (in)coherence of $\mathbf{A}$, which is defined as

$$\mu(\mathbf{A}) = \max_{1 \leq j < k \leq m} \frac{\langle A_j, A_k \rangle}{\|A_j\|_2 \|A_k\|_2}, \tag{3}$$

where A_i denotes the i-th column of $\mathbf{A}$, see [6, 14]. Some examples for matrices with small coherence can be found in [12].

In the radar setting, the sensing matrix $\mathbf{A}$ represents a physical process (the scattering of electromagnetic waves), and therefore we cannot simply choose $\mathbf{A}$ to be, say, a Gaussian random matrix or a random partial Fourier matrix. Nevertheless, certain parameters are under our control, such as the choice of the radar transmit signals, as well as the positions of the transmit and receive antennas. Therefore it is crucial to analyze whether and how the parameters under our control can be chosen such that that the MIMO radar sensing matrix has small coherence.

2 The Signal Model

Consider a MIMO radar employing N_T antennas at the transmitter and N_R antennas at the receiver. We assume that the element spacing is sufficiently small so that the radar return from a given scatterer is fully correlated across the array. In other words, this is a coherent propagation scenario.

To simplify the presentation we assume that the two arrays are co-located, i.e. this is a mono-static radar. The extension to the bi-static case is straightforward as long as the coherency assumption holds for each array. The arrays are characterized by the array manifolds: $\mathbf{a}_R(\theta)$ for the receive array and $\mathbf{a}_T(\theta)$ for the transmit array, where θ is the direction relative to the array. We assume that the arrays and all the scatterers are in the same 2-D plane. The extension to the 3-D case is straightforward and all of the following results hold for that case as well.

Let $\mathbf{Z}(t; \theta, r)$ be the $N_R \times N_s$ noise free received signal matrix from a unit strength target at direction θ and range r, where N_s is the number of samples in time. Then

$$\mathbf{Z}(t; \theta, r) = \mathbf{a}_R(\theta)\mathbf{a}_T^T(\theta)\mathbf{S}(t - \tau) \qquad (4)$$

where $\tau = 2r/c$, with c denoting the speed of light, and $\mathbf{S}(t - \tau)$ is a $N_T \times N_s$ matrix whose rows are the circularly delayed signals $s_i(t - \tau)$. The i-th transmit antenna transmits $s_i(t)$ where $t = 1, \cdots, N_s$.

Assuming uniformly spaced linear arrays (ULA), the array manifolds are given by

$$\mathbf{a}_T(\theta) = \begin{bmatrix} 1 \\ e^{j2\pi d_T \sin(\theta)} \\ \vdots \\ e^{j2\pi d_T \sin(\theta)(N_T-1)} \end{bmatrix} \qquad (5)$$

and

$$\mathbf{a}_R(\theta) = \begin{bmatrix} 1 \\ e^{j2\pi d_R \sin(\theta)} \\ \vdots \\ e^{j2\pi d_R \sin(\theta)(N_R-1)} \end{bmatrix} \qquad (6)$$

where d_T and d_R are the normalized spacings (distance divided by wavelength) between the elements of the transmit and receive arrays, respectively.

It is known that the spatial characteristics of a MIMO radar are closely related to that of a virtual array with $N_T N_R$ antennas, whose array manifold is $\mathbf{a}(\theta) = \mathbf{a}_T(\theta) \otimes \mathbf{a}_R(\theta)$. It is known [8] that the following choices for the spacing of the transmit and receive array spacing will yield a uniformly spaced virtual array with half wavelength spacing:

$$d_R = 0.5, d_T = 0.5N_R; \qquad (7)$$
$$d_T = 0.5, d_R = 0.5N_T. \qquad (8)$$

Both of these choices lead to a virtual array whose aperture is $0.5(N_T N_R - 1)$ wavelengths. This is the largest virtual aperture free of grating lobes. The choices (7) and (8) will also show up again in our theoretical analysis, see Theorem 1.

Next let $\mathbf{z}(t; \theta, r) = \vec{\mathbf{Z}}(t; \theta, r)$ be the noise-free vectorized received signal. We set up a discrete range-azimuth grid $\{(\theta_i, r_j)\}, 1 \leq i \leq N_\theta, 1 \leq j \leq N_r$, where Δ_θ and Δ_r denote the corresponding discretization stepsizes. Using vectors $\mathbf{z}(t; \theta, r)$ for all grid points (θ_i, r_j) we construct a complete response matrix $\mathbf{A}$ whose columns are $\mathbf{z}(t; \theta_i, r_j)$ for $1 \leq i \leq N_\theta$ and $1 \leq j \leq N_r$. In other words, we have N_r range values and N_θ azimuth values, so that $\mathbf{A}$ is a $N_R N_s \times N_r N_\theta$ matrix.

Assume that the radar illuminates a scene consisting of K scatterers located on K points of the (θ_i, r_j) grid. Let $\mathbf{x}$ be a sparse vector whose non-zero elements are the complex amplitudes of the scatterers in the scene. The zero elements corresponds to grid points which are not occupied by scatterers. We can then define the radar signal received from this scene $\mathbf{y}$ by

$$\mathbf{y} = \mathbf{A}\mathbf{x} + \mathbf{v} \qquad (9)$$

where $\mathbf{y}$ is a $N_R N_s \times 1$ vector, $\mathbf{x}$ is a $N_r N_\theta \times 1$ sparse vector, $\mathbf{v}$ is a $N_R N_s \times 1$ complex Gaussian noise vector, and $\mathbf{A}$ is a $N_R N_s \times N_r N_\theta$ matrix.

The discussion so far was for the case of a stationary radar scene and a fixed radar, in which case there is no Doppler shift. The extension of this signal model to include the Doppler effect is conceptually straightforward, but leads to a significant increase in the problem dimension.

The signal model for the return from a unit strength scatterer at direction θ, range r, and Doppler f_d (corresponding to its radial velocity with respect to the radar) is given by

$$\mathbf{Z}(t; \theta, r, f_d) = \mathbf{a}_R(\theta)\mathbf{a}_T^T(\theta)\mathbf{S}(t - \tau, f_d) \qquad (10)$$

where $\tau = 2r/c$, with c denoting the speed of light, and $\mathbf{S}(t - \tau)$ is a $N_T \times N_s$ matrix whose rows are the circularly delayed and Doppler shifted signals $s_i(t - \tau)e^{j2\pi f_d t}$.

As before we let $\mathbf{z}(t; \theta, r, f_d) = \vec{\mathbf{Z}}(t; \theta, r, f_d)$ be the noise-free vectorized received signal. We extend the discrete range-azimuth grid by adding a discretized Doppler component (with stepsize Δ_f and corresponding N_f Doppler values) and obtain a uniform range-azimuth-Doppler grid $\{(\theta_i, r_j, f_k)\}$. Using vectors $\mathbf{z}(t; \theta, r, f_d)$ for all discrete (θ_i, r_j, f_k) we construct a complete response matrix $\mathbf{A}$ whose columns are $\mathbf{z}(t; \theta_i, r_j, f_k)$ for $1 \leq i \leq N_\theta$, $1 \leq j \leq N_r$, $1 \leq k \leq N_f$.

Assume that the radar illuminates a scene consisting of K scatterers located on K points of the (θ_i, r_j, f_k) grid. Let $\mathbf{x}$ be a sparse vector whose non-zero elements are the complex amplitudes of the scatterers in the scene. The zero elements corresponds to grid points which are not occupied by scatterers. We can then define the radar signal received from this scene $\mathbf{y}$ by

$$\mathbf{y} = \mathbf{A}\mathbf{x} + \mathbf{v} \qquad (11)$$

where $\mathbf{y}$ is a $N_R N_s \times 1$ vector, $\mathbf{x}$ is a $N_r N_\theta N_f \times 1$ sparse vector, $\mathbf{v}$ is a $N_R N_s \times 1$ complex Gaussian noise vector, and $\mathbf{A}$ is a $N_R N_s \times N_r N_\theta N_f$ matrix.

3   Theoretical Results

Whether the system (11) is underdetermined or not depends on the the choice of the parameters $\Delta_\theta, \Delta_r, \Delta_f$. Clearly, we can always choose a very crude discretization of the radar scene and in that way ensure that (11) is overdetermined. But since we aim for high resolution in range, azimuth and Doppler, this is not the way to go. However when we increase the resolution (by making $\Delta_\theta, \Delta_r, \Delta_f$ small), we increase the number of columns of $\mathbf{A}$ and the linear system $\mathbf{A}\mathbf{x} = \mathbf{y}$ becomes more and more underdetermined. And at the same time the coherence of $\mathbf{A}$ becomes worse, since adjacent columns of $\mathbf{A}$ look more and more similar. Eventually $\mu(\mathbf{A})$ will become too large and Basis Pursuit will just fail. Thus we are facing a fundamental trade-off here and the key is to find the balance between maximal resolution and making sure that the

matrix $\mathbf{A}$ still satisfies the conditions under which Basis Pursuit will succeed.

The following theorem gives a flavor of the type of theoretical results we have derived. It addresses the case of a noise-free stationary radar scene. A similar, but slightly more involved, theorem holds for the Doppler case.

Theorem 1 *Assume we have N_T transmit antennas and N_R receive antennas with corresponding array manifolds given by (5) and (6). Assume further that we send a different AWGN signal of length N_s from each transmit antenna. Choose $d_R = \frac{1}{2}, d_T = \frac{1}{2}N_R$ or $d_R = \frac{1}{2}N_T, d_T = \frac{1}{2}$, let $-\pi/4 \leq \theta \leq \pi/4$, and set $\Delta_\tau = \frac{c}{2B}$ (where c is the speed of light and B is the signal bandwidth), $\Delta_\theta = \frac{2}{N_R N_T}$. Denote $N := \max\{N_R N_T, N_s\}$ and let $\varepsilon, \delta > 0$. Then s uniformly at random distributed targets of sparsity up to*

$$s < \frac{C_2 N_R N_s}{\ln \frac{N}{\delta} \ln \frac{N}{\varepsilon}}, \qquad C_2 > 0 \text{ is a constant}, \qquad (12)$$

can be recovered by Basis Pursuit with high probability (depending on ε, δ).

The proof, which is too long to be included here, will be presented in a forthcoming paper. The key idea of the proof is to show that the coherence of $\mathbf{A}$ is small, followed by applying Theorem B and Theorem 14 in [14]. Concerning the coherence of $\mathbf{A}$ we show that

$$\mu(\mathbf{A}) = \mathcal{O}\left(\min\left\{\frac{1}{\sqrt{N_R N_T}}, \frac{1}{\sqrt{N_s}}\right\}\right). \qquad (13)$$

To obtain the coherence (13) one needs to choose the values of d_R, d_T and Δ_θ as indicated in the theorem. Indeed, these choices are intimately related to the beampattern displayed in Figure 1.

In the noisy case we can replace (2) either by

$$\min_{\mathbf{x}} \|\mathbf{x}\|_1 \quad \text{s.t. } \|\mathbf{A}\mathbf{x} - \mathbf{y}\|_2 \leq \epsilon \qquad (14)$$

or by the equivalent Lasso [13]

$$\min_{\mathbf{x}} \frac{1}{2}\|\mathbf{A}\mathbf{x} - \mathbf{y}\|_2^2 + \lambda\|\mathbf{x}\|_1. \qquad (15)$$

A "noisy" analog of Theorem 1, using (15) instead of (2) can be derived by combining our coherence estimates for $\mathbf{A}$ with Theorem 1.2 in [1].

It seems likely, and is also indicated by our numerical simulations, that one can remove the requirement in Theorem 1 that the targets have to be randomly distributed.

4 Numerical Results

To illustrate the performance of the compressed sensing MIMO radar we present here a few "toy" examples. A more complete performance evaluation is beyond the scope of this paper and will be presented in a forthcoming paper. In these examples we use transmit and receive arrays with $N_T = N_R = 10$ elements and a spacing of $d_R = 0.5$, $d_T = 0.5N_R$. The number of azimuth-range samples are $N_\theta = 30$, $N_s = N_r = 30$.

Figure 1 depicts the beampattern of the virtual array which is seen to have a 3dB beamwidth of 1 deg which matches closely the reciprocal of the array aperture $0.5N_T N_R$. The width of the mainlobe from null-to-null is 2.3 deg. This array does not appear explicitly in the compressed sensing radar, but its beampattern is related to the achievable coherence of $\mathbf{A}$, and thus provides an indication of the expected spatial resolution of this radar system.
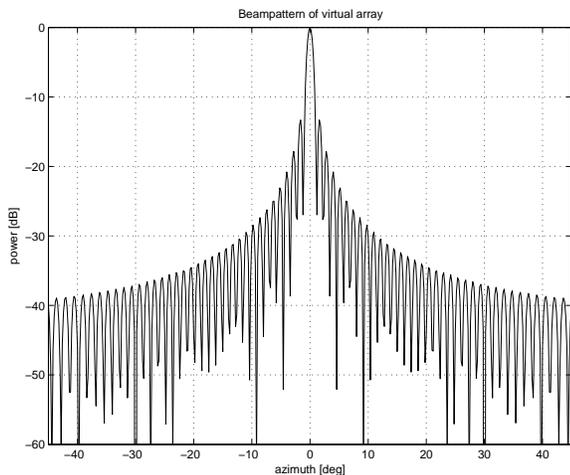
Figure 1. Beampattern of the virtual array, $N_T = N_R = 10$ **elements,** $d_R = 0.5$, $d_T = 0.5N_R$ **spacing, no windowing.**

Figure 2 depicts a radar scene consisting of 13 unit amplitude scatterers in a particular geometric arrangement. Note that in this example the targets are *not* randomly distributed. The sub-figure titled $\mathbf{X}$ shows the noise free radar scene. The sub-figure titled $\hat{\mathbf{X}}$ shows the estimated scene using the compressed sensing algorithm described above, using noisy data with noise standard deviation $\sigma = 3$. The third sub-figure is included for reference and shows the scene estimated using a matched filter, $\mathbf{X}_{mf}$. More precisely, $\mathbf{X}_{mf}$ is the reshaped version of the vector $\mathbf{x}_{mf}$,

$$\mathbf{x}_{mf} = \mathbf{W}^H \mathbf{x} \qquad (16)$$

where $\mathbf{W}$ is the matched filter matrix whose columns are the columns of $\mathbf{A}$ normalized to unit norm.
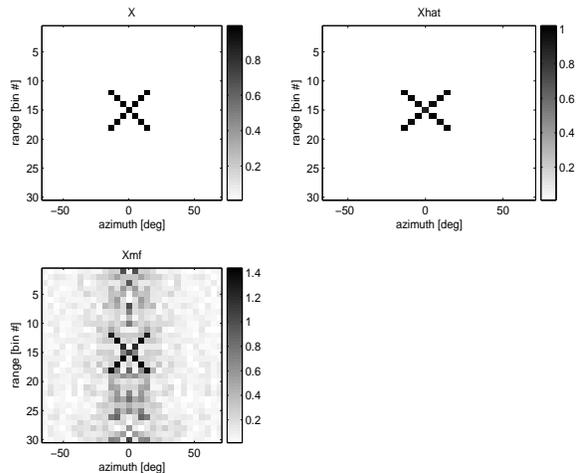
Figure 2. A radar scene X **with 13 scatterers, the estimated scene using the compressed sensing algorithm** $\hat{X}$ **and using a matched filter** X_{mf}**.**

Figure 3 depicts a radar scene consisting of 25 scatterers placed randomly and having amplitudes randomly distributed between 0 and 1. The sub-figure titled $\mathbf{X}$ shows the noise free radar scene. The sub-figure titled $\hat{\mathbf{X}}$ shows the estimated scene using the compressed sensing algorithm described above, using noisy data with noise standard deviation $\sigma = 3$. The third sub-figure is included for reference and shows the scene estimated using a matched filter, $\mathbf{X}_{mf}$.

Next we studied experimentally the level of sparsity at which the compressed sensing algorithm breaks down. As was shown in Theorem 1, the upper bound for the admissible sparsity s for $\mathbf{x}$ is roughly $\mathcal{O}(N_R N_s / \ln N)$. We generated random noise-free radar scenes for a given number of scatterers s and computed the average of the estimation error over these random scenes. The estimation error was defined as the Frobenius norm of $\mathbf{X} - \hat{\mathbf{X}}$. The experiment was repeated for different values of s and the results are depicted in figure 4. Note that the error is small for $s < 106$ and then increases rapidly for larger values of s. This behavior is in line with the well-known phase transition phenomenon for Gaussian and other compressed sensing matrices [7].
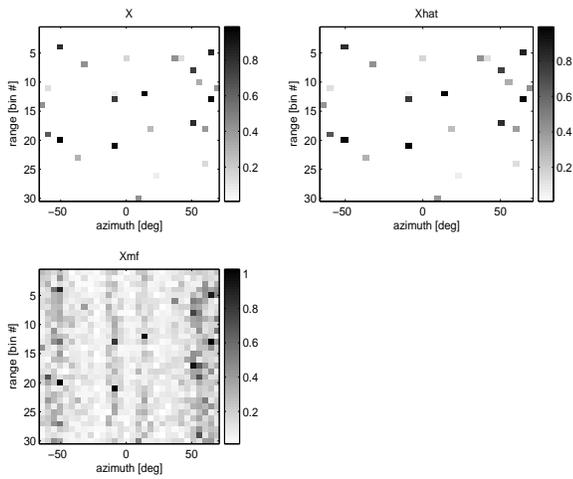
Figure 3. A random radar scene X with 25 scatterers, the estimated scene using the compressed sensing algorithm $\hat{\text{X}}$ and using a matched filter X_{mf}.
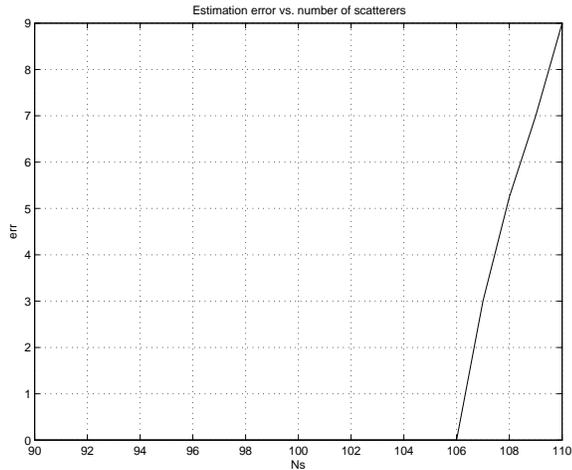
Figure 4. The average estimation error $\|\text{X} - \hat{\text{X}}\|$ for different numbers of scatterers s.

5 Conclusions

We have presented an initial theoretical and numerical framework for exploiting sparseness of radar scenes for MIMO radar. Based on results from compressed sensing we derive bounds on the achievable range- and azimuth resolution and the number of recoverable tar-

gets. Our theoretical and numerical findings indicate strong potential for using tools from sparse representations and compressive sensing for MIMO radar.

References

[1] E. J. Candès and Y. Plan. Near-ideal model selection by l1 minimization. *Annals of Statistics*, 37:2145–2177, 2009

[2] E. J. Candès, J. Romberg, and T. Tao. Robust uncertainty principles: Exact signal reconstruction from highly incomplete frequency information. *IEEE Trans. on Information Theory*, 52(2):489–509, 2006.

[3] E. J. Candès and T. Tao. Near-optimal signal recovery from random projections: Universal encoding strategies. *IEEE Trans. on Information Theory*, 52:5406–5425, 2006.

[4] C.Y. Chen and P. P. Vaidyanathan. Compressed Sensing in MIMO Radar. *Asilomar Conference on Signal, Systems, and Computers*, Pacific Grove, CA, Nov. 2008.

[5] D. L. Donoho. Compressed sensing. *IEEE Trans. on Information Theory*, 52(4):1289–1306, 2006.

[6] D. L. Donoho and X. Huo. Uncertainty principles and ideal atomic decompositions. *IEEE Trans. on Information Theory*, 47(7):2845–2862, 2001.

[7] D. L. Donoho and J. Tanner. Observed universality of phase transitions in high-dimensional geometry, with implications for modern data analysis and signal processing. *Philosophical Transactions of The Royal Society A*, 367(1906): 4273-4293, 2009.

[8] B. Friedlander, "On the relationship between MIMO and SIMO Radars," *IEEE Trans. Signal Processing*, vol. 57, no. 1, pp. 394–398, January 2009.

[9] B. Friedlander, "Adaptive Signal Design for MIMO Radar," chapter in *MIMO Radar Signal Processing*, J. Li and P. Stoica Eds., John Wiley & Sons, 2009.

[10] M. A. Herman and T. Strohmer, "High resolution radar via compressed sensing," *IEEE Transactions on Signal Processing,* vol. 57, no. 6, pp. 2275–2284, June 2009.

[11] B. Friedlander, "Waveform Design for MIMO Radars," *IEEE Transaction on Aerospace Electronic Systems*, vol. 43, no 3. pp. 1227-1238, July 2007.

[12] T. Strohmer and R. W. Heath Jr., "Grassmannian frames with applications to coding and communications," *Appl. Comp. Harm. Anal.*, vol.14(3): 257–275, 2003.

[13] R. Tibshirani. "Regression shrinkage and selection via the lasso". *J. Roy. Statist. Soc. Ser. B*, 58(1):267–288, 1996.

[14] J. A. Tropp. On the conditioning of random subdictionaries. Appl. Comput. Harmonic Anal., vol. 25, pp. 1–24, 2008.